

Aluminum Deoxidation Equilibria in Liquid Iron: Part II. Thermodynamic Modeling



MIN-KYU PAEK, JONG-JIN PAK, and YOUN-BAE KANG

Al deoxidation equilibria in liquid iron over the whole composition range from very low Al ([pct Al] = 0.0027) to almost pure liquid Al were thermodynamically modeled for the first time using the Modified Quasichemical Model in the pair approximation for the liquid phase. The present modeling is distinguished from previous approaches in many ways. First, very strong attractions between metallic components, Fe and Al, and non-metallic component, O, were taken into account explicitly in terms of Short-Range Ordering. Second, the present thermodynamic modeling does not distinguish solvent and solutes among metallic components, and the model calculation can be applied from pure liquid Fe to pure liquid Al. Therefore, this approach is thermodynamically self-consistent, contrary to the previous approaches using interaction parameter formalism. Third, the present thermodynamic modeling describes an integral Gibbs energy of the liquid alloy in the framework of CALPHAD; therefore, it can be further used to develop a multicomponent thermodynamic database for liquid steel. Fourth, only a small temperature-independent parameter for ternary liquid was enough to account for the Al deoxidation over wide concentration ($0.0027 < [\text{pct Al}] < 100$) and wide temperature range [1823 K to 2139 K (1550 °C to 1866 °C)]. Gibbs energies of Fe-O and Al-O binary liquid solutions at metal-rich region (up to oxide saturation) were modeled, and relevant model parameters were optimized. By merging these Gibbs energy descriptions with that of Fe-Al binary liquid modeled by the same modeling approach, the Gibbs energy of ternary Fe-Al-O solution at metal-rich region was obtained along with one small ternary parameter. It was shown that the present model successfully reproduced all available experimental data for the Al deoxidation equilibria. Limit of previously used interaction parameter formalism at high Al concentration is discussed.

DOI: 10.1007/s11663-015-0369-z

© The Minerals, Metals & Materials Society and ASM International 2015

I. INTRODUCTION

Al deoxidation equilibria in liquid iron-containing Al up to a few hundreds ppm have been the subject of intense interest for the production of normal Al-killed steels.^[1] Traditionally, the Wagner's Interaction Parameter Formalism (WIPF)^[2] has been very popular for the description of the equilibria at the low Al concentration region. A solid line in Figure 1 is a calculated deoxidation equilibria, using the WIPF recommended by the Japan Society for the Promotion of Science (JSPS).^[3] The predicted curve by the JSPS reproduced most experimental data shown by various symbols well at the low Al concentration region.^[1,4-7] However, the WIPF was neither validated at high Al concentration

region^[8-11] nor is, in principle, thermodynamically consistent.^[12] Therefore, its use at high Al concentration region should be carefully carried out, keeping in mind the above facts. Introducing second-order parameters proposed by Lupis and Elliott^[13] did not significantly improve the validity of the WIPF.

There are a number of inherent problems in the WIPF. First, it was originally formulated to be valid at infinite dilution, as indicated by Wagner himself.^[2] However, thanks to its mathematical simplicity, it has been very popular and has been used even at wider concentration range. In order for this formalism to be valid at wide concentration, the formalism should be at least quadratic,^[12,14] and special relationships among interaction parameters and Henrian activity coefficient should be obeyed.^[12,13,15] Second, the strong attraction force between Al and O in liquid iron was not taken into account properly. As discussed by Jung *et al.*,^[16] the WIPF inherently assumes random mixing among solutes such as Al and O, and their strong attraction force is described by very negative interaction parameters with large temperature dependence. They pointed out that such large temperature-dependent term is due to inappropriate evaluation of configurational entropy of mixing in the solution. They resolved the strong attraction between Al and O by introducing associates (Al^*O and Al_2^*O) in the framework of Unified Inter-

MIN-KYU PAEK, formerly Graduate Student with the Department of Materials Engineering, Hanyang University, ERICA, Ansan 426-791, Republic of Korea, is now Post-Doc. with the Department of Mining and Materials Engineering, McGill University, Montreal, QC H3A 2B2, Canada. JONG-JIN PAK, Professor, is with the Department of Materials Engineering, Hanyang University. YOUN-BAE KANG, Associate Professor, is with the Graduate Institute of Ferrous Technology, Pohang University of Science and Technology, Pohang, Kyungbuk 790-784, Republic of Korea. Contact e-mail: ybkang@postech.ac.kr

Manuscript submitted November 20, 2014.

Article published online May 19, 2015.

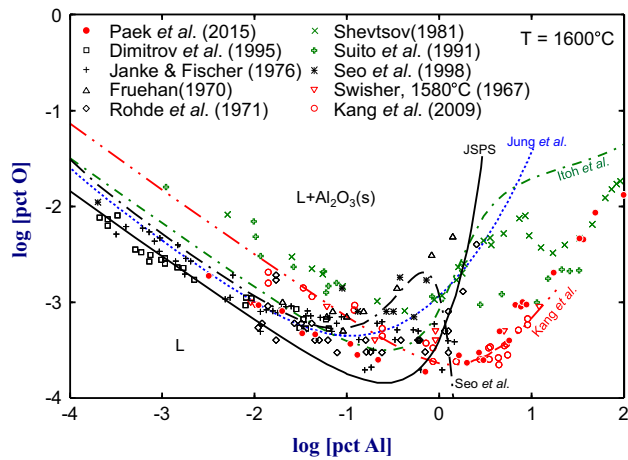


Fig. 1—Experimental data (symbols) and thermodynamic calculations (lines) for the Al deoxidation equilibria in liquid iron at 1873 K (1600 °C), available in literatures^[1,3–11,16,57] as well as those of the present authors' experimental data.^[33] “L” represents the liquid Fe-Al-O alloy.

action Parameter Formalism (UIPF), which is a modification of WIPF to be thermodynamically consistent at high concentration. They have had significantly improved description of deoxidation equilibria, not only for Al but also for other alloying elements such as Ca, Mg, Mn, Si, *etc.* However, due to inherent limit of the interaction parameter formalism, its applicability is limited only at low Al region.

In order to further resolve the problems mentioned above, the CALculation of PHase Diagram (CALPHAD)-type approach was employed where the deoxidation equilibria are described by a chemical equilibrium between liquid alloy (Fe-Al-O) and solid oxide (Al_2O_3). Contrary to the WIPF where activity coefficient was mainly concerned, in the present study, integral Gibbs energy of the liquid alloy was a main function to be described. In this way, the activity coefficient of solute is obtained by differentiation, and thermodynamic consistency between the activity coefficients is always guaranteed. Depending on the validity of the integral Gibbs energy, the validity of the activity coefficient derived subsequently is also assured.

In the present study, thermodynamic modeling covers from pure liquid Fe to pure liquid Al and toward oxide saturation limit. This means that the present model calculation can be applied in metal-rich solution with no limit of Al content. In order to take into account the strong Short-Range Ordering (SRO) mainly between Al and O and Fe and O, the Modified Quasichemical Model (MQM) in the pair approximation^[17,18] was used. In the present study, by the thermodynamic calculation, the Al deoxidation equilibria in liquid iron were described over the whole composition range for the first time.

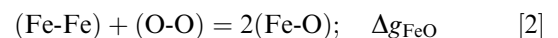
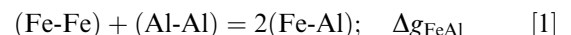
For the thermodynamic modeling of the liquid Fe-Al-O solution, its sub-systems (Fe-Al, Fe-O, and Al-O) should be first modeled. In the current study, the Fe-O binary liquid at Fe-rich region was modeled using available experimental data such as the O solubility^[19–25] and the O activity data^[26–32] in liquid iron. Similarly for the Al-O

binary liquid, O solubility limit in the pure Al liquid was experimentally measured by the present authors as described Part I of the present series.^[33] Regarding the Fe-Al binary solution, in the present authors' recent study,^[34] it was found that thermodynamic description of binary Fe-Al system available in literature^[35,36] did not properly account for the enthalpy of mixing in the binary liquid solution. Thus, the liquid solution property has been re-optimized using MQM,^[34] and the model parameters were directly used in the current study. By combining the optimized model parameters of the three sub-binary solutions, the Gibbs energy of the ternary liquid solution was estimated. In the present article, the procedure of thermodynamic modeling in each binary system is described. Model calculation for the Al deoxidation equilibria in liquid iron is shown along with all available experimental data including those of the present authors'.^[33] Extension of the current study to include Mn, both by experiment and thermodynamic modeling, will be reported in Part III of the present series.^[37] All the calculations and optimizations in the present study were performed with the FactSage thermochemical software.^[38]

II. THERMODYNAMIC MODEL USED IN THE PRESENT STUDY

The liquid alloy composed of Fe-Al-O was modeled using the MQM in the pair approximation, in order to take into account the SRO exhibited in the liquid solution over a wider concentration range. Modeling SRO in liquid solutions by the MQM has been well demonstrated.^[39,40] Detailed description of the MQM and its associated notations are available in References 17 and 18. Gibbs energies of pure liquid Fe, Al, and O were taken from Dinsdale.^[41] Gibbs energies of solid Al_2O_3 and liquid Fe_xO were taken from Eriksson *et al.*^[42] and Deckerov *et al.*,^[43] respectively.

For the present ternary Fe-Al-O liquid alloy, the following three pair exchange reactions are considered in the pair:



where (*i-j*) represents a First-Nearest Neighbor (FNN) pair. There are total six types of pairs. The non-configurational Gibbs energy change for the formation of two moles of (*i-j*) pairs is Δg_{ij} . Let n_i and n_j be the number of moles of *i* and *j*, n_{ij} be the number of moles of (*i-j*) pairs, and Z_i be the coordination numbers of *i*. Then, the following mass balance equations for the pairs are obtained.

$$Z_{\text{Fe}}n_{\text{Fe}} = 2n_{\text{FeFe}} + n_{\text{FeAl}} + n_{\text{FeO}} \quad [4]$$

$$Z_{\text{Al}}n_{\text{Al}} = 2n_{\text{AlAl}} + n_{\text{FeAl}} + n_{\text{AlO}} \quad [5]$$

$$Z_{\text{O}n\text{O}} = 2n_{\text{OO}} + n_{\text{FeO}} + n_{\text{AlO}} \quad [6]$$

The pair fractions, mole fractions, and “coordination-equivalent” fractions are defined respectively as:

$$X_{ij} = n_{ij}/(n_{\text{FeFe}} + n_{\text{AlAl}} + n_{\text{OO}}) \quad [7]$$

$$X_i = n_i/(n_{\text{Fe}} + n_{\text{Al}} + n_{\text{O}}) \quad [8]$$

$$\begin{aligned} Y_i &= Z_i n_i / (Z_{\text{Fe}} n_{\text{Fe}} + Z_{\text{Al}} n_{\text{Al}} + Z_{\text{O}} n_{\text{O}}) \\ &= Z_i X_i / (Z_{\text{Fe}} X_{\text{Fe}} + Z_{\text{Al}} X_{\text{Al}} + Z_{\text{O}} X_{\text{O}}) \end{aligned} \quad [9]$$

The Gibbs energy of the Fe-Al-O ternary liquid alloy is given by:

$$\begin{aligned} G &= (n_{\text{Fe}} g_{\text{Fe}}^{\circ} + n_{\text{Al}} g_{\text{Al}}^{\circ} + n_{\text{O}} g_{\text{O}}^{\circ}) - T \Delta S^{\text{config}} \\ &+ (n_{\text{FeAl}}/2) \Delta g_{\text{FeAl}} + (n_{\text{FeO}}/2) \Delta g_{\text{FeO}} + (n_{\text{AlO}}/2) \Delta g_{\text{AlO}} \end{aligned} \quad [10]$$

where g_{Fe}° , g_{Al}° , and g_{O}° are the molar Gibbs energies of pure liquid Fe, Al, and O, respectively, and they are taken from SGTE data compilation by Dinsdale.^[41] ΔS^{config} is an approximate expression for the configurational entropy of mixing given by randomly distributing the six different types of pairs in the one-dimensional Ising approximation:^[17]

$$\begin{aligned} \Delta S^{\text{config}} &= -R(n_{\text{Fe}} \ln X_{\text{Fe}} + n_{\text{Al}} \ln X_{\text{Al}} + n_{\text{O}} \ln X_{\text{O}}) \\ &- R \left[\begin{aligned} &n_{\text{FeFe}} \ln \left(\frac{X_{\text{FeFe}}}{Y_{\text{Fe}}^2} \right) + n_{\text{AlAl}} \ln \left(\frac{X_{\text{AlAl}}}{Y_{\text{Al}}^2} \right) + n_{\text{OO}} \ln \left(\frac{X_{\text{OO}}}{Y_{\text{O}}^2} \right) \\ &+ n_{\text{FeAl}} \ln \left(\frac{X_{\text{FeAl}}}{2Y_{\text{Fe}} Y_{\text{Al}}} \right) \\ &+ n_{\text{FeO}} \ln \left(\frac{X_{\text{FeO}}}{2Y_{\text{Fe}} Y_{\text{O}}} \right) + n_{\text{AlO}} \ln \left(\frac{X_{\text{AlO}}}{2Y_{\text{Al}} Y_{\text{O}}} \right) \end{aligned} \right] \end{aligned} \quad [11]$$

Δg_{ij} may be expanded in terms of the pair fractions^[18]:

$$\begin{aligned} \Delta g_{\text{FeAl}} &= \Delta g_{\text{FeAl}}^{\circ} + \sum_{k \geq 1} g_{\text{FeAl}}^{k0} \left(\frac{X_{\text{FeFe}}}{X_{\text{FeFe}} + X_{\text{AlAl}} + X_{\text{FeAl}}} \right)^k \\ &+ \sum_{l \geq 1} g_{\text{FeAl}}^{0l} \left(\frac{X_{\text{AlAl}}}{X_{\text{FeFe}} + X_{\text{AlAl}} + X_{\text{FeAl}}} \right)^l \end{aligned} \quad [12]$$

$$\Delta g_{\text{FeO}} = \Delta g_{\text{FeO}}^{\circ} \quad [13]$$

$$\Delta g_{\text{AlO}} = \Delta g_{\text{AlO}}^{\circ} \quad [14]$$

where Δg_{ij}° , g_{ij}^{k0} , and g_{ij}^{0l} are the parameters of the model which can be functions of temperature. Although the Δg_{FeO} and Δg_{AlO} may be expressed as functions of the pair fractions as was done for Δg_{FeAl} , such complexity was not required in the present study because the present study concerns only dilute O concentration.

The equilibrium pair distribution is calculated by setting:

$$(\partial G / \partial n_{\text{FeAl}})_{n_{\text{Fe}}, n_{\text{Al}}, n_{\text{O}}} = 0 \quad [15]$$

$$(\partial G / \partial n_{\text{FeO}})_{n_{\text{Fe}}, n_{\text{Al}}, n_{\text{O}}} = 0 \quad [16]$$

$$(\partial G / \partial n_{\text{AlO}})_{n_{\text{Fe}}, n_{\text{Al}}, n_{\text{O}}} = 0 \quad [17]$$

This gives three equilibrium constants for the following quasichemical reactions of Eqs. [1] through [3]:

$$\frac{X_{\text{FeAl}}^2}{X_{\text{FeFe}} X_{\text{AlAl}}} = 4 \exp \left(- \frac{\Delta g_{\text{FeAl}}}{RT} \right) \quad [18]$$

$$\frac{X_{\text{FeO}}^2}{X_{\text{FeFe}} X_{\text{OO}}} = 4 \exp \left(- \frac{\Delta g_{\text{FeO}}}{RT} \right) \quad [19]$$

$$\frac{X_{\text{AlO}}^2}{X_{\text{AlAl}} X_{\text{OO}}} = 4 \exp \left(- \frac{\Delta g_{\text{AlO}}}{RT} \right) \quad [20]$$

There are six unknowns (n_{FeFe} , n_{AlAl} , n_{OO} , n_{FeO} , n_{AlO} , and n_{FeAl}) for a given set of n_{Fe} , n_{Al} , and n_{O} , and six equations (Eqs. [4] through [6], [18] through [20]). These are solved in order to get the equilibrium number of moles of the six pairs. Those can be back substituted into the Eqs. [10] and [11] with the help of the Eqs. [7] through [9], in order to obtain the G . By the principle of Gibbs energy minimization of the whole system (the liquid Fe-Al-O alloy and a solid Al_2O_3), the equilibrium concentration of the liquid solution can be obtained.

The composition of maximum SRO in each binary subsystem is determined by ratio of the coordination numbers, Z_i/Z_j , as given each of them by the following equations:

$$\frac{1}{Z_i} = \frac{1}{Z_{ii}^i} \left(\frac{2n_{ii}}{2n_{ii} + n_{ij}} \right) + \frac{1}{Z_{ij}^i} \left(\frac{n_{ij}}{2n_{ii} + n_{ij}} \right) \quad [21]$$

$$\frac{1}{Z_j} = \frac{1}{Z_{jj}^j} \left(\frac{2n_{jj}}{2n_{jj} + n_{ij}} \right) + \frac{1}{Z_{ji}^j} \left(\frac{n_{ij}}{2n_{jj} + n_{ij}} \right), \quad [22]$$

where Z_{ii}^i and Z_{ij}^i are the values of Z_i , respectively, when all nearest neighbors of an i are i 's, and when all nearest neighbors of an i are j 's, and where Z_{ij}^j and Z_{ji}^j are defined similarly. Z_{ij}^i and Z_{ji}^i represent the same quantity and can be used interchangeably. The coordination numbers for all pure elements (Z_{ii}^i) were set to 6. Coordination numbers in binary Fe-Al solution ($Z_{\text{FeAl}}^{\text{Fe}}$, $Z_{\text{FeAl}}^{\text{Al}}$) are 6,^[34] while those in binary Fe-O ($Z_{\text{FeO}}^{\text{Fe}}$, $Z_{\text{FeO}}^{\text{O}}$) and Al-O ($Z_{\text{AlO}}^{\text{Al}}$, $Z_{\text{AlO}}^{\text{O}}$) solutions were set to 2 in order to consider the higher degree of ordering.^[17] These choices were made to best represent the data, and the values of the coordination numbers selected in the current study are listed in Table I.

Gibbs energy of the ternary solution estimated in this way could reproduce most available experimental data as close as possible, even without any ternary adjustable parameter. Nevertheless, in order to refine the model

Table I. Model Parameters Optimized or Used for the Fe-Al-O Ternary Liquid Alloy in the current Study (J/mol)

Liquid (L)—MQM (Fe, Al, O)	
$Z_{\text{FeFe}}^{\text{Fe}} = Z_{\text{AlAl}}^{\text{Al}} = Z_{\text{OO}}^{\text{O}} = Z_{\text{FeAl}}^{\text{Fe}} = Z_{\text{FeAl}}^{\text{Al}} = 6$	
$Z_{\text{FeO}}^{\text{Fe}} = Z_{\text{FeO}}^{\text{O}} = Z_{\text{AlO}}^{\text{Al}} = Z_{\text{AlO}}^{\text{O}} = 2$	
$g_{\text{Fe}}, g_{\text{Al}}, g_{\text{O}}$	From ^[41]
Δg_{FeO}	$-142,867 + 8.37T$
Δg_{AlO}	$-464,633 + 96.65T$
Δg_{FeAl}	$-20,292.4 + 3.347T - (1673.6 + 1.255T)X_{\text{FeFe}} - 1046X_{\text{FeFe}}^2 - (10,460 - 4.184T)X_{\text{AlAl}}$ ^[34]
$g_{\text{AlO(Fe)}}^{001}$	$-16,736$

calculation for better fitting, a small ternary parameter, $g_{\text{AlO(Fe)}}^{001}(Y_{\text{Fe}}/(Y_{\text{Fe}} + Y_{\text{Al}}))$, was added to the Eq. [14]. All optimized model parameters determined in the current study are listed in Table I.

III. RESULTS AND DISCUSSION

The present study aims at thermodynamic modeling of the Fe-Al-O liquid up to oxide saturation limit for the deoxidation equilibria. Therefore, maximum O content shall be generally less than 1 mass pct. Modeling including liquid oxide phase is out of scope in the present study.

A. Fe-O Binary Liquid

For the binary Fe-O liquid, there are two types of experimental data available: solubility and chemical potential of O in liquid iron. Solubility limit of O in liquid iron in equilibrium with liquid Fe oxide (Fe_xO) is shown in Figure 2,^[19–25] and oxygen partial pressure exerted on the liquid Fe-O alloy at various temperatures is shown in Figure 3.^[26–32] The O solubility in liquid iron was measured by the various experimental techniques. The O solubility determined in some earlier investigations^[19–21] might have been contaminated by refractory crucible. As the iron oxide melts below 1773 K (1500 °C), it was inevitable to use other refractory materials such as alumina or magnesia. In order to overcome this difficulty, a rotating crucible technique^[22] or a levitation melting technique^[23–25] has been used. However, as shown in Figure 2, the reported data of O solubility in liquid iron in equilibrium with liquid iron oxide, Fe_xO , scattered significantly. Even with the levitation melting where the liquid Fe-O metallic alloy was in contact with only with liquid Fe_xO , due to low interfacial tension between the two phases, portion of the Fe_xO might have been penetrated into the liquid Fe and have resulted in overestimation of O content. Therefore, a lower O content among reported data may be preferred. On the other hand, oxygen isobars over liquid Fe-O alloy controlled by $\text{H}_2/\text{H}_2\text{O}$ equilibration or measured by EMF techniques shown in Figure 3 are generally in good agreement. As all these data are relevant to dilute O region, only $\Delta g_{\text{FeO}}^\circ$ term (independent on composition but temperature dependent) was used to reproduce these data, mainly to have better

agreement with the data shown in Figure 3. This was because these oxygen isobars correspond to the homogeneous solution property of the liquid alloy, and they are relatively in agreement each other. As a result, the calculated solubility limit of O in the liquid alloy locates at lower [pct O] as shown by a line in Figure 2. This is also reasonable in the view of possibility of Fe_xO contamination into liquid Fe-O alloy.

B. Al-O Binary Liquid

The Al-O binary system has been extensively reviewed by Wriedt.^[44] He mentioned that no credible measurement of O solubility in liquid Al alloy was found. For the assessment of this system, he used the evaluated O solubility^[45] from the enthalpies and entropies of solution of O. Later, Taylor *et al.*^[46] determined the Gibbs energy of solution of O in the pure Al melt by adopting the correlation between the O solubility proposed by Fitzner *et al.*^[47] and the enthalpy and entropy of solution tabulated in the JANAF thermochemical database.^[48] According to their assessments, the O solubility in liquid Al alloy in equilibrium with solid Al_2O_3 was predicted. However, no experimental measurement has been reported up to date.

In Part I of the present series, the present authors reported the O solubility limit in pure Al melt in equilibrium with solid Al_2O_3 in the temperature range from 1673 K to 1873 K (1400 °C to 1600 °C). In order to reduce analytical error of the O content in the alloy, CaO flux was added on top of the alloy. The added CaO flux reacted with primary Al_2O_3 inclusions, melted, and absorbed the Al_2O_3 particles, effectively. The residual inclusions in the melt were identified as pure solid Al_2O_3 , and the activity of Al_2O_3 was assumed to be unity. Therefore, the measured O content was considered as the O solubility limit in the liquid Al melt in equilibrium with Al_2O_3 .

As shown in Figure 4, the average values of the present experimental results were used to optimize model parameter of the MQM in the current study. As was done for the Fe-O binary liquid solution, only $\Delta g_{\text{AlO}}^\circ$ term (independent on composition but temperature dependent) was used. The calculated result shown by a line is in good agreement with the present experimental data.^[33] This is also in good accordance with the prediction by Taylor *et al.*^[46]'s result.

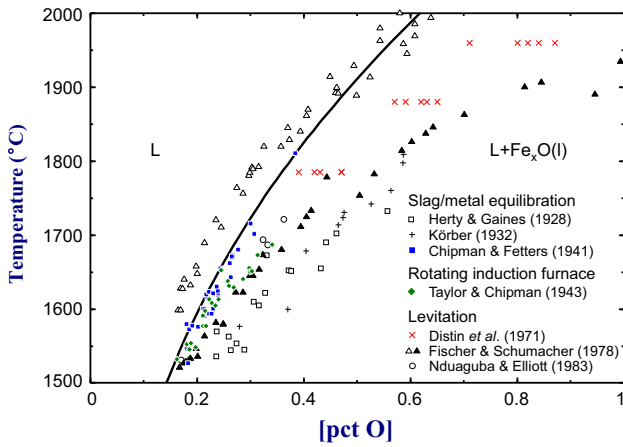


Fig. 2—O solubility in liquid iron in equilibrium with liquid Fe_xO . Symbols are reported experimental data,^[19–25] and line is the calculated in the present study.

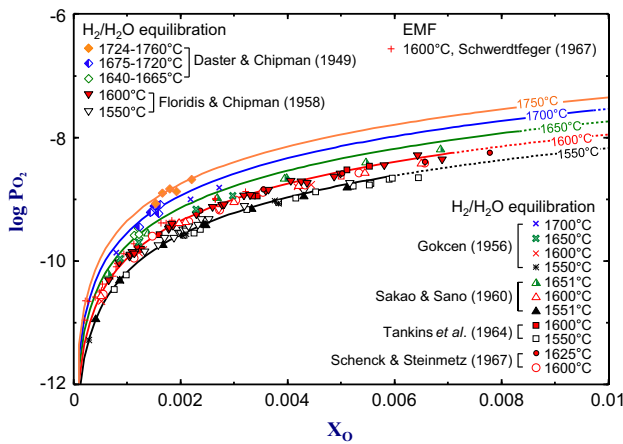


Fig. 3—Oxygen partial pressure over liquid iron calculated by the present model (lines) along with experimental data.^[26–32] Dotted lines represent the calculated oxygen partial pressure for undercooled liquid.

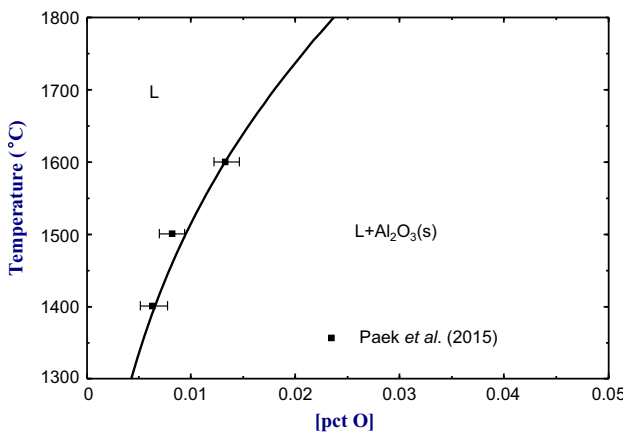


Fig. 4—O solubility in pure Al melt in equilibrium with Al_2O_3 . Symbols are experimental data measured by the present authors in Part I,^[33] and the line is the calculated solubility in the present study.

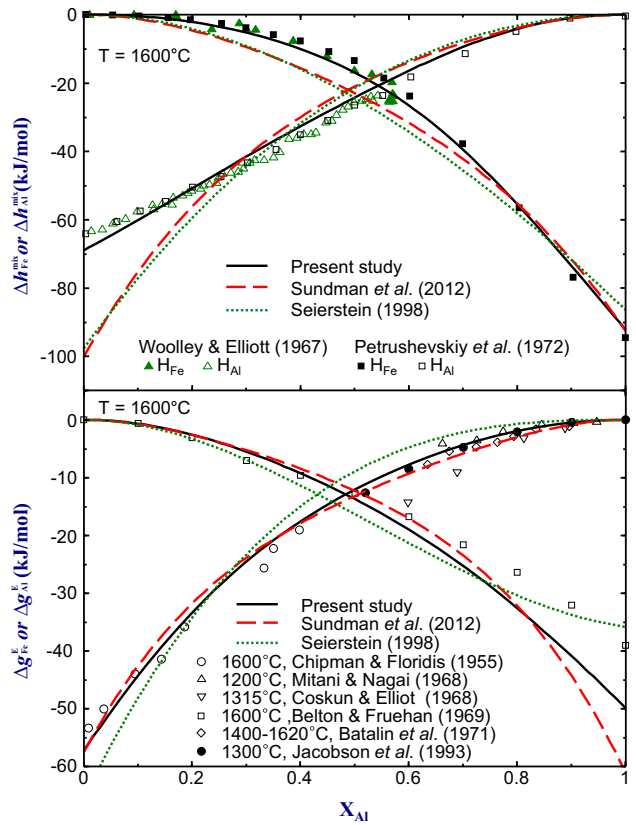


Fig. 5—Partial enthalpy and partial excess Gibbs energy of mixing in liquid Fe-Al alloys at 1873 K (1600 °C)^[35,36,51–56] along with the present authors recent optimization^[34] and previous modeling.^[49,50]

C. Fe-Al Binary Liquid

Gibbs energy of binary Fe-Al solution has been evaluated previously^[49,50] using a random mixing model. However, in the present authors' recent study,^[34] it was found that the enthalpy of mixing in the liquid Fe-Al phase calculated from previous thermodynamic modelings^[49,50] was not consistent with the experimental results reported in the literature.^[35,36] As shown in Figure 5, the partial Gibbs energies of mixing calculated by the previous modeling (a dashed line^[49] and a dotted line^[50]) are in good agreement with the available experimental data.^[51–56] However, the partial enthalpy of mixing of the previous investigations is significantly exothermic than the experimental data. This means that partial entropy of mixing is also more negative in these calculations, and the activity coefficient of Al in Fe-rich region may be well accounted for by these models at 1873 K (1600 °C) but will be less accurate at the other temperature. This discrepancy was identified and was revised by the present authors.^[34] In the revision of the binary Fe-Al system, the MQM was also used to model the liquid phase. The new thermodynamic calculation is shown as solid line in Figure 5, showing better agreement with the experimental results. The reoptimization can affect the individual contributions of enthalpy and entropy to the Gibbs energy of liquid phase as well as the stability of all the solid phases in this system.^[34]

D. Deoxidation in Fe-Al-O Ternary Liquid

The Al deoxidation equilibria in liquid iron have been reported by several researchers by experiment and thermodynamic calculation.^[1,3–11,16,57] As mentioned in Section I, no reliable thermodynamic calculation over wide composition range, in particular for high Al concentration region, has been reported. This is, as discussed, mainly because of neglecting the SRO between Al and O and limit of the interaction parameter formalism to cover wide concentration range. In the present study, the Gibbs energy of liquid Fe-Al-O solution which encompasses from Fe to Al and takes into account the SRO was used to calculate the Al deoxidation equilibria. In Figure 6, the calculation at 1873 K (1600 °C) using the MQM in the present study is shown along with the available experimental data^[1,4–11] including those measured by the present authors^[33] at 1873 K (1600 °C). Only using the model descriptions in each binary system, the Al deoxidation equilibria in the ternary system were predicted as shown by a dashed line. The agreement is generally good. At low Al content below 0.1 mass pct, the prediction without any ternary parameter agrees well with the experimental data of Janke and Fischer,^[5] Dimitrov *et al.*,^[6] Seo *et al.*,^[7] and those of the present authors.^[33] Between $0.1 < [\text{pct Al}] < 10$, the prediction estimates the equilibrium O content slightly lower than the experimental data. However, it should be noted that the O content is indeed in the range of single ppm where the analytical uncertainty is as large as the analyzed value of the O content. When $[\text{pct Al}] > 10$, the prediction estimates slightly lower $[\text{pct O}]$ than the experimental data (Suito *et al.*,^[11] Shevtsov,^[10] and present authors^[33]). The discrepancy is generally less than 10 ppm. This is a remarkable result for the prediction of Al deoxidation equilibria over wide concentration range *without* any adjustable fitting parameter. Nevertheless, in order to fit the reported experimental data more precisely, one small adjustable ternary parameter was introduced in the current study. With the ternary parameter, the Al deoxidation equilibria were calculated as shown by a solid line. The agreement was improved.

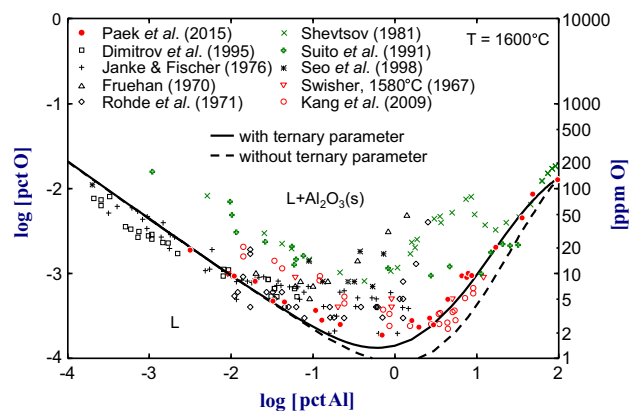


Fig. 6—Al deoxidation equilibria in liquid iron at 1873 K (1600 °C). A dashed line is the predicted equilibria without any ternary parameter. A solid line is the calculated deoxidation equilibria with a ternary parameter.

In the WIPF, the interaction parameter, e_{O}^{Al} , represents a ternary interaction between Al and O in Fe. This parameter is a main measure to describe the Al deoxidation equilibria. In practice, not only this first-order parameter but also second-order parameters were used to calculate the deoxidation equilibria, but only with limited success. On the other hand, the present analysis shows that a proper consideration of solution behavior could result in better prediction for the deoxidation equilibria, even with no ternary parameter. Introducing the small ternary parameter played only a minor role in fine tuning of the calculation. This lends a strong support to the modeling approach used in the current study.

Using the same model equation and parameters, the Al deoxidation equilibria were calculated above 1873 K up to 2139 K (1600 °C up to 1866 °C) where experimental data were available. All the calculations and the experimental data are shown in Figure 7. By only introducing the temperature-independent ternary parameter, the experimental data at high temperature could also be very well reproduced. This is contrary to the use of a large temperature-dependent term in WIPF for the first-order interaction parameter ($e_{\text{O}}^{\text{Al}} = -20,600/T + 7.15$ ^[58]). It is thought that the excess entropy of mixing naturally considered in the quasichemical approximation (second term in the Eq. [11]) partly contributes to the improved description for the deoxidation equilibria in the present thermodynamic modeling. This emphasizes the necessity of the proper consideration of the SRO for the calculation of deoxidation equilibria in liquid iron. Importance of the SRO in the modeling of liquid in general point of view has been discussed previously.^[39,40]

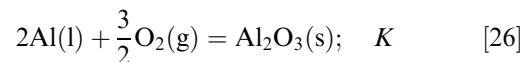
Figure 8 shows oxygen partial pressure in liquid alloy at Al_2O_3 saturation, as a function of the Al content. Gas/solid/alloy equilibration techniques with known gas composition ($\text{H}_2/\text{H}_2\text{O}$) or EMF technique were previously used in order to determine activity of O in liquid alloy^[4–6,59] or equilibrium oxygen partial pressure over the liquid alloy.^[60,61] The activity of O was converted to the oxygen partial pressure as follows^[62]:

$$\frac{1}{2}\text{O}_2(\text{g}) = \underline{\text{O}}; \quad \Delta G_{[23]}^\circ = -117,152 - 2.89T(\text{J/mol}) \quad [23]$$

$$K = \frac{h_{\text{O}}}{P_{\text{O}_2}^{1/2}} = \frac{f_{\text{O}}[\text{pct O}]}{P_{\text{O}_2}^{1/2}} = \exp\left(\frac{-\Delta G_{[23]}^\circ}{RT}\right) \quad [24]$$

$$P_{\text{O}_2} = (f_{\text{O}}[\text{pct O}])^2 \exp\left(\frac{2\Delta G_{[23]}^\circ}{RT}\right) \quad [25]$$

The oxygen partial pressure decreases as Al content increases:



$$\log P_{O_2} = -\frac{4}{3}\log h_{Al} - \frac{2}{3}\log K = -\frac{4}{3}\log[\text{pct Al}] - \frac{2}{3}(2\log f_{Al} + \log K) \quad [27]$$

The activity coefficient of Al, f_{Al} , is approximated to be 1 when Al content is low enough that h_{Al} is approximated to be [pct Al]. Therefore, up to 1 mass pct of [pct Al], linear decrease of oxygen partial pressure is seen with the slope $-4/3$, regardless of temperature. This is no more true at high Al content because f_{Al} increases rapidly as Al content increases.

It is further to be noted that, as can be seen from the EMF data of Dimitrov *et al.*,^[6] addition of flux or type of crucibles used had little effect on the partial pressure of oxygen (activity of O). This is a clear evidence of the local equilibrium between liquid and Al_2O_3 , which was imposed in the present authors' experimental study.^[33]

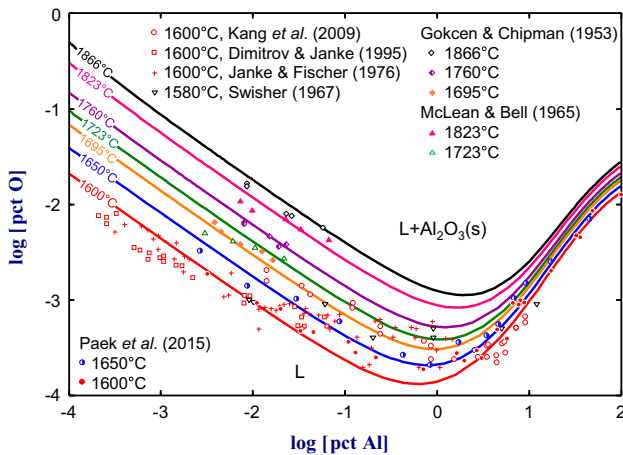


Fig. 7—Comparison between experiments^[5,6,8,9,33,60,61] and model calculations for Al deoxidation equilibria in the liquid iron at various temperature from 1873 K to 2139 K (1600 °C to 1866 °C).

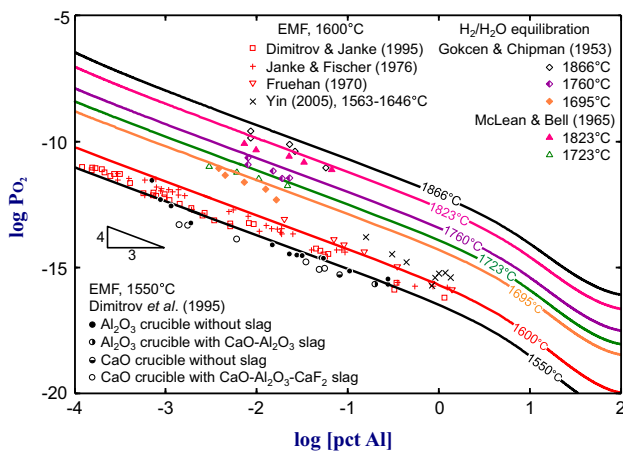


Fig. 8—Calculated O partial pressure in Fe-Al-O melts along with experimental results.^[4-6,59-61]

E. Thermodynamics of Deoxidation Described by MQM and WIPF

Activity coefficient of O, f_O at 1873 K (1600 °C), in practically used 1 mass pct standard state, in liquid Fe-Al-O in equilibrium with Al_2O_3 was calculated by the MQM with the optimized model parameter in the current study and the WIPF along with available interaction parameters.^[1,3,58] In the case of the MQM, using the relationship given in Eq. [23] and [25], the f_O was calculated from the oxygen partial pressure (Figure 8) and [pct O] (Figure 6) values by the MQM. In the calculation, the following information was used^[41]:

$$O(l) = 1/2O_2(g); \Delta G_{[28]}^\circ = 2648.9 - 31.44T(\text{J/mol}), \quad [28]$$

where the activity of O with respect to the pure liquid O is direct output of the model calculation.

This is shown as a solid line in Figure 9, and the f_O gradually decreases as Al content increases and approaches to a value which corresponds to the activity coefficient of O in pure liquid Al, with respect to 1 mass pct standard state in liquid Fe. The derived f_O is considered to be reliable as was evidenced by the previous figures (Figures 6, 7, and 8).

On the other hand, the f_O can also be calculated using the WIPF by the following equation:

$$\log f_O = e_O^O[\text{pct O}] + e_O^{Al}[\text{pct Al}] + r_O^{Al}[\text{pct Al}]^2 + r_O^{Al,O}[\text{pct Al}][\text{pct O}] \quad [29]$$

along with the reported interaction parameters.^[1,3,58] The $\log f_O$ calculated using only the first-order interaction parameters recommended by JSPS^[3] linearly decreased with an increasing Al content, as expected from the mathematical form of Eq. [29]. This clearly indicates that this formula can only be used in very limited concentration range. Introducing the second-order interaction parameters, for example, those available in the compilation of Sigworth and Elliott,^[58] does

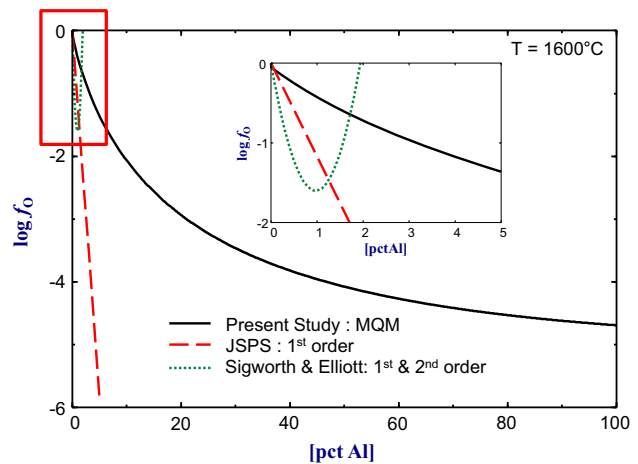


Fig. 9—Comparison between calculated $\log f_O$ in Fe-Al-O melts by MQM (solid line) and Wagner's formalism^[1,3,58] (dashed and dotted line) at 1873 K (1600 °C).

not improve the results. Other choices of the first/second-order interaction parameters do not lead significantly better accordance with that of the present study. This indicates that the quadratic form of Eq. [29] may be used, but only limited concentration region.

It is very interesting that Holcomb and Pierre proposed to use an exponential function for the f_O as^[63]:

$$\log f_O = e_O^{\text{Al}}(1 - \exp(-\kappa[\text{pct Al}]))/\kappa, \quad [30]$$

where κ is a model parameter used in their study.

Their proposed form of f_O varies similar to what is shown in Figure 9 by the MQM in such a way that f_O monotonously decreases as Al content increases, approaching to a value (approximately e_O^{Al}/κ). However, Eq. [30] is based on no physical basis, while the present study is based on a theoretical background.

The equilibrium O content obtained in the present model calculation is a result of sum of oxygen in various FNN pairs containing O ((Fe-O), (Al-O), and (O-O)). Therefore, it is interesting to observe the distribution of various pairs. The (Al-O) may be seen in such a way that O in liquid alloy is tightly bound by Al. The same holds for (Fe-O). The (O-O) may represent dissolved O with no FNN metallic component. The calculated pair fractions of various pairs in the liquid Fe-Al-O alloy in equilibrium with Al_2O_3 at 1873 K (1600 °C) are

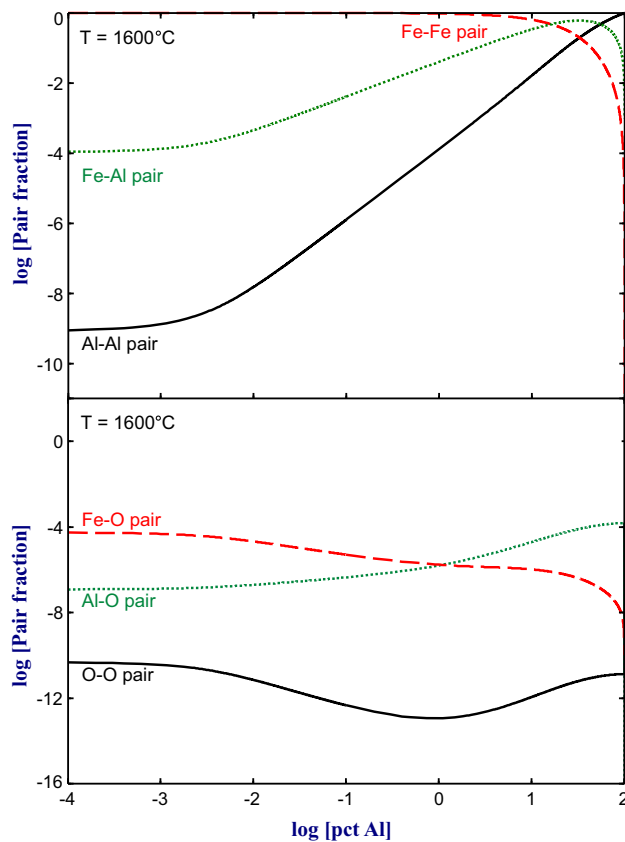


Fig. 10—Predicted pair fractions of various pairs in liquid Fe-Al-O in equilibrium with Al_2O_3 at 1873 K (1600 °C).

shown in Figure 10. When [pct Al] is low, most O is represented by the (Fe-O) pair, and this gradually decreases as Al content increases. On the other hand, the increase of [pct Al] increases the (Al-O) pair. Fraction of the (O-O) pair is very low and does not contribute to the equilibrium O content significantly. The distribution of these pairs, giving the minimum Gibbs energy at a given composition though the three equations (Eqs. [15] through [17]), looks reasonable and are well accordance with the equilibrium O content. It is expected that the present modeling approach applies not only for the Al deoxidation equilibria but also deoxidation by other elements. In the next article of the present series (Part III),^[37] it will be shown that the same modeling approach can also be applied to describe deoxidation by Mn in liquid iron, and the model prediction will be shown for the high Mn-high Al-containing steels. And this will be validated by experimental data including the present authors' own work.

IV. CONCLUSIONS

In order to thermodynamically analyze the Al deoxidation equilibria in liquid iron over the wide composition/temperature range, the liquid solution of the Fe-Al-O system was thermodynamically modeled using the MQM. It was emphasized that the present modeling approach is not limited by Al content, thereby one can predict equilibrium O content from pure liquid Fe to pure liquid Al. The deoxidation equilibria in the Fe-Al-O system were successfully described for a wide composition/temperature range only with a small temperature-independent ternary parameter. This was attributed to the fact that the strong attractions between components were treated explicitly in terms of SRO. Solubility and partial pressure of oxygen in Fe-O and Al-O binary alloys were fitted to the model equation. Along the solution property of Fe-Al binary liquid, Al deoxidation in the liquid Fe-Al-O alloy was calculated and compared with reliable experimental data including the present authors' own measurement up to pure liquid Al. The agreement between the model calculation and experimental data was very good. It was shown that the traditional approach assuming random mixing of solutes in the framework of interaction parameter formalism is not appropriate to be applied over wide concentration range. The present thermodynamic model can be extended to model the multicomponent steel solution, for example, including Mn to describe the complex deoxidation equilibria in the high Mn-high Al-alloyed liquid steels.

ACKNOWLEDGMENT

This study was supported by a Grant (NRF-2013K2A2A2000634) funded by the National Research Foundation of Korea, Republic of Korea.

NOMENCLATURE

Δg_{ij}	Gibbs energy change for the formation of two moles of (<i>i-j</i>) pairs (J/mol)
ΔS^{config}	Configurational entropy of mixing (J/mol K)
[pct <i>i</i>]	Mass percent of <i>i</i> (–)
a_i	Raoultian activity of <i>i</i> (–)
e_i^j	Wagner's first-order interaction parameter of <i>j</i> on <i>i</i> (–)
f_i	Henrian activity coefficient of <i>i</i> in mass pct scale (–)
g_i°	Molar Gibbs energy of pure component <i>i</i> (J/mol)
h_i	Henrian activity of <i>i</i> in mass pct scale (–)
K	The equilibrium constant (–)
n_i	Number of moles of <i>i</i> (mol)
n_{ij}	Number of moles of (<i>i-j</i>) pairs (mol)
R	Gas constant (8.314 J/mol K)
r_i^j	Wagner's second-order interaction parameter of <i>j</i> on <i>i</i> (–)
T	Absolute temperature (K)
X_i	Mole fraction of <i>i</i> (–)
X_{ij}	Pair fraction of (<i>i-j</i>) pairs (–)
Y_i	Coordination-equivalent fraction of <i>i</i> (–)
Z_i	Coordination number of <i>i</i> (–)
Z_{ij}^i	Coordination number of <i>i</i> in <i>i-j</i> binary solution when all nearest neighbors of an <i>i</i> are <i>j</i> 's
κ	Holcomb and Pierre's model parameter for the exponential function, ^[63] (–)
MQM	Modified Quasichemical Model
SRO	Short-Range Ordering
CALPHAD	CALCulation of PHase Diagram
WIPF	Wagner's Interaction Parameter Formalism
JSPS	Japan Society for the Promotion of Science
UIPF	Unified Interaction Parameter Formalism
FNN	First-Nearest Neighbor
EMF	Electro Motive Force

REFERENCES

1. L.E. Rohde, A. Choudhury, and M. Wahlster: *Arch. Eisenhüttenwes.*, 1971, vol. 42, pp. 165–74.
2. C. Wagner: *Thermodynamics of Alloys*, Addison-Wesley Press, Cambridge, MA, 1952, pp. 47–51.
3. The 19th Committee in Steelmaking: *Thermodynamic Data For Steelmaking*, The Japan Society for Promotion of Science, Tohoku University Press, Sendai, Japan, 2010, pp. 10–13.
4. R.J. Fruehan: *Metall. Trans.*, 1970, vol. 1, pp. 3403–10.
5. D. Janke and W.A. Fischer: *Arch. Eisenhüttenwes.*, 1976, vol. 47, pp. 195–98.
6. S. Dimitrov, A. Weyl, and D. Janke: *Steel Res.*, 1995, vol. 66, pp. 3–7.
7. J.D. Seo, S.H. Kim, and K.R. Lee: *Steel Res.*, 1998, vol. 69, pp. 49–53.
8. J.H. Swisher: *Trans. Metall. Soc. AIME*, 1967, vol. 239, pp. 123–24.
9. Y.J. Kang, M. Thunman, D. Sichen, T. Morohoshi, K. Mizukami, and K. Morita: *ISIJ Int.*, 2009, vol. 49, pp. 1483–89.
10. V.E. Shevtsov: *Russ. Metall.*, 1981, vol. 1, pp. 52–57.
11. H. Suito, H. Inoue, and R. Inoue: *ISIJ Int.*, 1991, vol. 31, pp. 1381–88.
12. L.S. Darken: *Trans. AIME*, 1967, vol. 239, pp. 80–89.
13. C.H.P. Lupis and J.F. Elliott: *Acta Metall.*, 1960, vol. 14, pp. 529–38.
14. A.D. Pelton: *Metall. Mater. Trans. B*, 1997, vol. 28B, pp. 869–76.
15. S. Srikanth and K.T. Jacob: *Metall. Trans. B*, 1988, vol. 19B, pp. 269–75.
16. I.H. Jung, S.A. Decterov, and A.D. Pelton: *Metall. Mater. Trans. B*, 2004, vol. 35B, pp. 493–507.
17. A.D. Pelton, S.A. Decterov, G. Eriksson, C. Robelin, and Y. Dessureault: *Metall. Mater. Trans. B*, 2000, vol. 31B, pp. 651–59.
18. A.D. Pelton and P. Chartrand: *Metall. Mater. Trans. A*, 2001, vol. 32A, pp. 1355–60.
19. H. Herty and J.M. Gaines: *Trans. AIME*, 1928, vol. 80, pp. 142–56.
20. F. Korber: *Stahl und Eisen*, 1932, vol. 52, pp. 133–44.
21. J. Chipman and K.L. Fetters: *Trans. Am. Soc. Met.*, 1941, vol. 29, pp. 953–67.
22. C.R. Taylor and J. Chipman: *Trans. AIME*, 1943, vol. 154, pp. 228–47.
23. P.A. Distin, S.G. Whiteway, and C.R. Masson: *Can. Metall. Q.*, 1971, vol. 10, pp. 13–18.
24. W.A. Fischer and J.F. Schumacher: *Arch. Eisenhüttenwes.*, 1978, vol. 49, pp. 431–35.
25. M. Nduaguba and J.F. Elliott: *Metall. Trans. B*, 1983, vol. 14B, pp. 679–83.
26. M.N. Dastur and J. Chipman: *Met. Trans.*, 1949, vol. 185, pp. 441–45.
27. N.A. Gokcen: *Trans. AIME*, 1956, vol. 206, pp. 1558–67.
28. T.P. Floridis and J. Chipman: *Trans. Metall. Soc. AIME*, 1958, vol. 212, pp. 549–53.
29. H. Sakao and K. Sano: *Trans. JIM*, 1960, vol. 1, pp. 38–42.
30. E.S. Tankins, N.A. Gokcen, and G.R. Belton: *Trans. Metall. Soc. AIME*, 1967, vol. 230, pp. 820–27.
31. V.H. Schenck and E. Steinmetz: *Arch. Eisenhüttenwes.*, 1967, vol. 38, pp. 813–19.
32. K. Schwerdtfeger: *Trans. Metall. Soc. AIME*, 1967, vol. 239, pp. 1276–81.
33. M.K. Paek, J.M. Jang, Y.-B. Kang, and J.J. Pak: *Metall. Mater. Trans. B*, 2015. DOI:10.1007/s11663-015-0368-0.
34. A.T. Phan, M.K. Paek, and Y.-B. Kang: *Acta Mater.*, 2014, vol. 79, pp. 1–15.
35. F. Wooley and J.F. Elliot: *Trans. AIME*, 1967, vol. 239, pp. 1872–83.
36. M.S. Petrushevsky, Yu.O. Esin, P.V. Gel'd, and V.M. Sandakov: *Russ. Metall.*, 1972, vol. 6, pp. 149–53.
37. M.K. Paek, K.H. Do, Y.-B. Kang, I.H. Jung, and J.J. Pak: unpublished research, 2015.
38. C.W. Bale, E. Bélisle, P. Chartrand, S.A. Decterov, G. Eriksson, K. Hack, I.H. Jung, Y.-B. Kang, J. Melançon, A.D. Pelton, C. Robelin, and S. Petersen: *CALPHAD*, 2009, vol. 33, pp. 295–311.
39. A.D. Pelton and Y.-B. Kang: *Int. J. Mater. Res.*, 2007, vol. 98, pp. 907–17.
40. Y.-B. Kang and A.D. Pelton: *CALPHAD*, 2010, vol. 34, pp. 180–88.
41. A.T. Dinsdale: *CALPHAD*, 1991, vol. 15, pp. 317–425.
42. G. Eriksson and A.D. Pelton: *Metall. Trans. B*, 1993, vol. 24B, pp. 807–16.
43. S.A. Decterov, E. Jak, P.C. Hayes, and A.D. Pelton: *Metall. Mater. Trans. B*, 2001, vol. 32B, pp. 643–57.
44. H.A. Wriedt: *Bull. Alloy Phase Diagr.*, 1985, vol. 6, pp. 548–53.
45. S. Otsuka and Z. Kozuka: *J. Jpn. Inst. Met.*, 1981, vol. 22, p. 558.
46. J.R. Taylor, A.T. Dinsdale, M. Hillert, and M. Selleby: *CALPHAD*, 1992, vol. 16, pp. 173–79.
47. K. Fitzer: *Thermochem. Acta*, 1982, vol. 52, pp. 103–11.
48. M.W. Chase, Jr: *NIST-JANAF Thermochemical Tables*, AIP, Woodbury, NY, 1998.
49. M. Seiersten: in *COST 507: Thermochemical Database for Light Metal Alloy*, 1998, vol. 2.
50. B. Sundman, I. Ohnuma, N. Dupin, U.R. Kattner, and S.G. Fries: *Acta Mater.*, 2009, vol. 57, pp. 2896–2908.
51. J. Chipman and T.P. Floridis: *Acta Metall.*, 1955, vol. 3, pp. 456–59.
52. H. Mitani and H. Nagai: *J. Jan. Inst. Met.*, 1968, vol. 32, pp. 752–55.

53. A. Coskun and J.F. Elliott: *Trans. Metall. Soc. AIME*, 1968, vol. 242, pp. 253–55.
54. G.R. Belton and R.J. Fruehan: *Trans. Metall. Soc. AIME*, 1969, vol. 245, pp. 113–17.
55. G.I. Batalin, E.A. Beloborodova, V.A. Stukalo, and L.V. Goncharuk: *Russ. J. Phys. Chem.*, 1971, vol. 45, pp. 1139–40.
56. N.S. Jacobson and G.M. Nehrotra: *Metall. Trans. B*, 1993, vol. 24B, pp. 481–86.
57. H. Itoh, M. Hino, and S. Banya: *Tetsu-to-Hagané*, 1997, vol. 83, pp. 773–78.
58. G.K. Sigworth and J.F. Elliott: *Met. Sci.*, 1974, vol. 8, pp. 298–310.
59. H. Yin: *Proc. of Int. Conf. of AISTech 2005*, Warrendale, PA, 2005, vol. 2, pp. 89–97.
60. N.A. Gokcen and J. Chipman: *J. Met.*, 1953, vol. 197, pp. 173–78.
61. A. McLean and H.B. Bell: *J. Iron Steel Inst.*, 1965, vol. 203, pp. 123–30.
62. E.T. Turkdogan: *Physical Chemistry of High Temperature Technology*, Academic Press, New York, 1980, p. 81.
63. G.R. Holcomb and G.R. St. Pierre: *Metall. Trans. B*, 1992, vol. 23B, pp. 789–90.